J. Fluid Mech. (1980), *vol.* 101, *part* 2, *pp.* 321–348
Printed in Great Britain

Long nonlinear waves in stratified shear flows

By S. A. MASLOWE
Mathematics Department, McGill University,
Montreal, P.Q. H3A 2K6

AND L. G. REDEKOPP
Department of Aerospace Engineering,
University of Southern California,
Los Angeles, California 90007

(Received 20 September 1979 and in revised form 6 March 1980)

The propagation of finite-amplitude internal waves in a shear flow is considered for wavelengths that are long compared to the shear-layer thickness. Both singular and regular modes are investigated, and the equation governing the amplitude evolution is derived. The theory is generalized to allow for a radiation condition when the region outside the stratified shear layer is unbounded and weakly stratified. In this case, the evolution equation contains a damping term describing energy loss by radiation which can be used to estimate the persistence of solitary waves or nonlinear wave packets in realistic environments. A continuous three-layer model is studied in detail and closed-form expressions are obtained for the phase speed and the coefficients of the nonlinear and dispersive terms in the amplitude equation as a function of Richardson number.

1. Introduction

The propagation of nonlinear surface waves whose length is great compared to the depth of the water has been studied extensively over the past century. Interest in the problem has been particularly strong during the last decade owing to the recently discovered properties of solitons. Analogous phenomena can occur in the context of long nonlinear *internal* waves, but the associated theory has, until recently, received relatively less attention. It is only now becoming recognized that such waves are likely to occur rather frequently both in the atmosphere and the oceans. Their existence requires that some feature of the basic flow profile or surroundings acts as a horizontal waveguide. This effect may be produced by either a nearby horizontal boundary or else a layer of moderately stratified fluid, above and below which the fluid is homogeneous by comparison. The latter situation is commonplace, for example in the oceanic thermocline and in the region of atmospheric fronts. There is also generally a significant amount of shear present in such an environment. Yet, previous studies have for the most part ignored shear in the mean flow and, therefore, our principal objective here is to investigate its influence.

The early studies of long nonlinear internal waves dealt with two-layer systems confined between horizontal boundaries and date back to the theoretical and experimental work of Keulegan (1953). Peters & Stoker (1960) seem to have been the first

0022-1120/80/4573-2390 $02.00

to consider solitary waves in a continuously stratified fluid. A convenient perturbation procedure for dealing with this class of problems was presented by Benney (1966), who applied his formulation to surface waves on a shear flow, internal waves and Rossby waves. The end result in each case was that the amplitude evolved according to the Korteweg–de Vries (KdV) equation

$$A_\tau + \alpha A A_\xi + \beta A_{\xi\xi\xi} = 0. \tag{1.1}$$

Here, the perturbation stream function has been expressed in the form

$$\psi = A(\xi, \tau)\,\phi(y),$$

where τ is a slow time scale and ξ describes slow spatial modulations in a co-ordinate system moving at the linear wave speed. The constants α and β are a property of the specific flow under consideration and their determination often requires a considerable computational effort.

A significant advance in the study of long nonlinear internal waves took place in 1967 with the concurrent appearance of papers by Benjamin and Davis & Acrivos dealing with the case where the fluid depth is large compared to an embedded wave guide scale. The long-wave limit of the linear dispersion relation is different in this case, leading to a modified form of the KdV equation in which the linear dispersive term is replaced by an integral. The equation can be written as

$$A_\tau + \gamma A A_\xi + \delta \frac{\partial^2}{\partial \xi^2}\left\{\frac{1}{\pi} \int_{-\infty}^{\infty} \frac{A(\xi', \tau)}{\xi - \xi'} d\xi'\right\} = 0, \tag{1.2}$$

and we shall refer to it as the mdKdV equation.† A most important contribution of Benjamin was to find a simple closed-form solitary wave solution to this nonlinear integro-differential equation. An N-soliton solution of (1.2) has been found recently by Chen, Lee & Pereira (1979) and by Matsuno (1979).

The form of the dispersive term for intermediate ratios of the wave-guide scale to the fluid column depth has been derived by Kubota, Ko & Dobbs (1978) and special solutions and properties of the resulting amplitude equation have been presented by Joseph (1977) and by Satsuma, Ablowitz & Kodama (1980). However, we consider only the two limiting cases for which (1.1) and (1.2) are applicable.

As noted above, there is reason to believe that the long waves under discussion are significant in the context of geophysical fluid dynamics. Internal solitons, in the absence of shear, are stable and very easy to generate in the laboratory as was originally pointed out by Davis & Acrivos. This suggests that they ought to be observable in the oceans and atmosphere and, in fact, a number of tentative observations have been reported in the literature. For example, Christie, Muirhead & Hales (1978) have published microbarograph data indicating the occurrence of solitary waves over central Australia in a variety of circumstances. Similarly, it is likely that long or solitary internal waves were present in the satellite observations of oceanic wave-packets reported by Apel *et al.* (1975). Certainly, the longer of these waves ought to be describable by a theory such as the one presented here, because the wavelengths

† This acronym, denoting the modified dispersive KdV equation, is chosen because the equation describes the balance between the leading-order nonlinear and dispersive terms in the long-wave limit. We prefer to designate the class of equations possessing this balance as being of KdV type.

were as much as 40 times the relevant vertical length scale. Some nonlinear features were noted by Apel *et al.* and, indeed, the measured amplitudes were great enough for one to expect that to be the case.

Although simultaneous measurements of shear were not available, there was reason to believe in each of these cases that a significant shear was present. For example, the satellite observations of internal wave packets were correlated with semidiurnal and diurnal tides at the edge of the continental shelf. Farmer & Smith (1978) report measurements of internal solitary waves in Knight Inlet, British Columbia, and emphasize that the waves were propagating in a strongly sheared flow. In the atmospheric case, Christie *et al.* discuss a number of possible generating mechanisms, finally concluding that the observed solitary waves were associated with sea-breeze currents. While attempting to make comparisons between their data and the theoretical work available at the time, these authors (p. 817) state, 'Perhaps the most serious criticisms of the direct application of these models to nonlinear wave propagation in the earth's atmosphere are the neglect of wind shear and the over-simplification of the fluid density structure'. Obviously, we agree.

Before commenting on the density structure, we should note that a start has been made in assessing the influence of shear in a paper by Lee & Beardsley (1974). These authors examined only the KdV limit (flow between horizontal boundaries), treating a two-layer case in some detail. However, in their discussion of the continuous case, they failed to consider the possibility of singular modes (i.e. modes having a critical point where the phase speed is equal to the mean flow velocity). Such modes can exist at $O(1)$ Richardson numbers provided that nonlinear effects, rather than diffusive effects, dominate in the critical-layer region. This was demonstrated by Maslowe (1973) who obtained a numerical solution for a stratified mixing layer. In § 3 of the present paper this point is made more explicitly in that singular long-wave solutions are obtained in closed form. Thus the present study, in many respects, parallels the work of Redekopp (1977) who investigated Rossby wave solitons. In that case as well, both regular and singular neutral-mode solutions are possible and a nonlinear critical-layer analysis was employed to obtain a uniformly valid solution.

Returning now to the subject of the density profile, previous studies have assumed the outer region in the unbounded case to be homogeneous. However, that is generally not the case in the real atmosphere and oceans, and that fact turns out to be most pertinent in the long-wave theory. It is shown below that for a given non-zero value of the Brunt–Väisälä frequency there is a definite restriction placed upon the minimum value of the amplitude for which permanent waves are possible. A particularly interesting case occurs when the stratification is small enough so that permanent nonlinear waves can occur, but a radiation condition applies in the outer region. Additional terms must then be included in (1.2) and these have the effect of a linear damping mechanism. This result is not surprising in retrospect because it is known from other problems that a radiation condition acts in the same manner as a small dissipative term. The derivation of the requisite evolution equation for this case is presented in § 2.2 and the damping characteristics for a solitary wave are discussed in § 4.

2. Derivation of the amplitude equations

We consider two-dimensional motion of a Boussinesq fluid for which the equations of motion are

$$\nabla . \mathbf{q} = 0, \quad \mathbf{q} = \{u_s(z)+u, w\},$$

$$\rho_t + (\mathbf{q}.\nabla)\rho + w\rho_s'(z) = 0,$$

$$\mathbf{q}_t + (\mathbf{q}.\nabla)\mathbf{q} = -\nabla\left(\frac{p}{\rho_0}\right) - \hat{\mathbf{e}}_z g \frac{\rho}{\rho_0}.$$

The undisturbed hydrostatic state with the ambient density distribution $\rho_s(z)$ and a horizontal, parallel shear flow $u_s(z)$ has been removed in these equations. Hence ρ denotes the local departure of the fluid density from the ambient and ρ_0 is a constant reference density used in the Boussinesq approximation. We introduce non-dimensional variables by scaling time with N_0^{-1}, where N_0 is a reference value (the maximum, say) of the Brunt–Väisälä frequency, space co-ordinates with L, a typical vertical scale associated with the stratified shear layer, scaling velocities with $N_0 L$, and scaling the perturbation buoyancy $(g\rho/\rho_0)$ by $N_0^2 L$. Then, after defining a stream-function and buoyancy variable by

$$\left.\begin{aligned} \Psi &= \int_{z_c}^{z} \{U(z')-c\}\,dz' + \epsilon\psi(x,z,t), \\ u &= \psi_z, \quad w = -\psi_x, \end{aligned}\right\} \tag{2.1a}$$

$$\frac{g\rho/\rho_0}{N_0^2 L} = \epsilon\sigma(x,z,t), \tag{2.1b}$$

the equations of motion can be written in the form

$$\{\partial_t + (U-c)\,\partial_x + \epsilon(\psi_z\partial_x - \psi_x\partial_z)\}\,\sigma + N^2(z)\,\psi_x = 0, \tag{2.2}$$

$$\{\partial_t + (U-c)\,\partial_x + \epsilon(\psi_z\partial_x - \psi_x\partial_z)\}\,\nabla^2\psi - U''\psi_x = \sigma_x. \tag{2.3}$$

The perturbed flow, with non-dimensional amplitude $0 < \epsilon \ll 1$, is referenced to a co-ordinate system moving with the linear, long-wave phase speed c. All variables in these equations are non-dimensional and the mean shear flow $U(z)$ has the definition

$$U(z) = \frac{U_0}{N_0 L}\frac{u_s}{U_0} = FV(z), \tag{2.4}$$

where U_0 is a measure of the velocity difference across the shear layer. In most of the following discussion we consider situations where the internal Froude number $F \sim O(1)$, but reference to the limit $F \downarrow 0$ will be made at several points to make connexion with previous results for unsheared environments. Although the form of the velocity profile $V(z)$ is kept arbitrary in the following derivations, the scale of the sheared layer is assumed to be no greater than that of the stratified layer so that the local Richardson number is everywhere greater than one-quarter.

2.1. *Shallow-water theory: the KdV equation*

We discuss first the case where the stratified shear flow is bounded above and below by rigid, horizontal planes with a separation distance of the same order as L. Then, if the wavelength is long compared to the shear flow, it is also long compared to the fluid depth and the usual KdV theory prevails (albeit with due consideration of the critical-layer region where the phase speed c is equal to the local flow velocity at some level z_c, say).

If, for the moment, we restrict the discussion to a single mode without a critical layer, it is straightforward to show that the asymptotic solution for $\epsilon \downarrow 0$ in which the leading-order effects of nonlinearity and dispersion are balanced is given by

$$\psi = A(\xi, \tau)\,\phi(z) + \epsilon\{A_{\xi\xi}\phi_d^{(2)}(z) + \tfrac{1}{2}A^2\,\phi_n^{(2)}(z)\} + \dots, \tag{2.5a}$$

$$\sigma = A\theta(z) + \dots = -A\frac{N^2\phi}{U-c} + \dots. \tag{2.5b}$$

The quantities $\phi(z)$ and c are determined from the eigenvalue problem

$$\mathscr{L}\phi \equiv \phi'' - \frac{U''}{U-c}\phi + \frac{N^2}{(U-c)^2}\phi = 0, \quad \phi(z_1) = \phi(z_2) = 0, \tag{2.6}$$

and $A(\xi, \tau)$ satisfies the KdV equation (1.1). The slow space and time scales for the amplitude function $A(\xi, \tau)$ are

$$\xi = \epsilon^{\frac{1}{2}}x, \quad \tau = \epsilon^{\frac{3}{2}}t. \tag{2.7}$$

The 1:3 ratio between the space and time scales derives from the linear dispersion relation and the $\epsilon^{\frac{1}{2}}$ scale for ξ emerges from the requirement that the effects of non-linearity and dispersion contribute at the same order in the expansion. The coefficients α and β in the KdV equation are determined by solvability conditions on the in-homogeneous equations

$$\mathscr{L}\phi_d^{(2)} = -\phi - \beta\frac{2N^2 - U''(U-c)}{(U-c)^3}\phi, \tag{2.8}$$

$$\mathscr{L}\phi_n^{(2)} = \frac{\phi^2}{(U-c)^4}\{U'''(U-c)^2 - U''U'(U-c) - 2(U-c)(N^2)' + 3U'N^2\} - \alpha\frac{2N^2 - U''(U-c)}{(U-c)^3}\phi. \tag{2.9}$$

These equations have homogeneous boundary conditions at $z = z_1, z_2$. Therefore, the coefficients are

$$\alpha = \frac{1}{I_1}\int_{z_1}^{z_2}\frac{\phi^3}{(U-c)^4}\{U'''(U-c)^2 - U''U'(U-c) - 2(U-c)(N^2)' + 3U'N^2\}\,dz, \tag{2.10a}$$

and

$$\beta = -\frac{1}{I_1}\int_{z_1}^{z_2}\phi^2\,dz, \tag{2.10b}$$

where

$$I_1 = \int_{z_1}^{z_2}\frac{\phi^2}{(U-c)^3}[2N^2 - U''(U-c)]\,dz. \tag{2.10c}$$

Observe that the coefficient α vanishes if there is no shear *and* if N is constant. In this limit the nonlinearity derives from the non-Boussinesq terms which are neglected here (cf. Benjamin 1966, Long 1965). Either a weak shear or non-constant Brunt–Väisälä frequency distribution are sufficient to contribute a quadratic nonlinear term to the amplitude evolution equation even when the variable density effects are neglected in the inertial terms. In most practical cases these effects are more significant than the small non-Boussinesq terms.

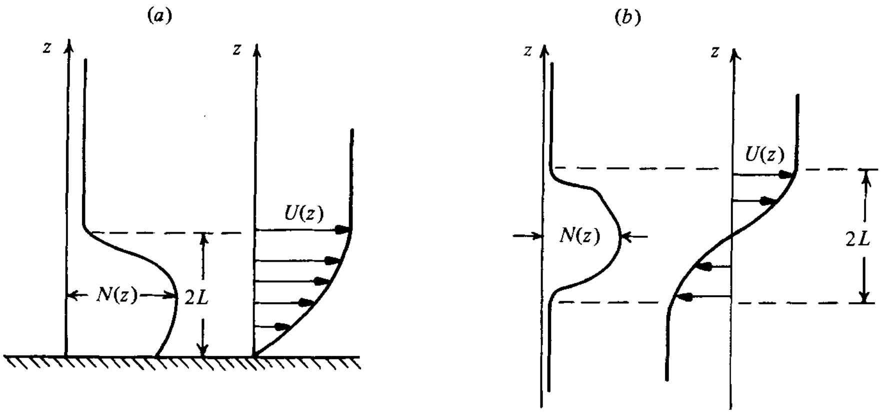

FIGURE 1. Flow models of unbounded stratified shear flows.

When a critical layer is present, some of the integrals in (2.10) do not exist and a modified solvability condition must be employed (cf. Redekopp 1977). The theory carries through leading to the same amplitude evolution equation providing the nonlinearity is sufficiently strong for all times within the critical-layer region. This is discussed further in § 2.3 and analytic results are obtained for singular neutral modes in a specific-shear flow in § 3.

2.2. *Deep-water theory: the mdKdV equation*

Let us now consider the case where the stratified shear flow with vertical scale L exists in an unbounded fluid domain. The fluid outside this wave guide is assumed to be unsheared and only weakly stratified. We have in mind flow configurations such as those shown in figure 1. The analysis will address the configuration shown in figure 1 (*a*). Calculations for specific cases of both configurations will be presented in § 3.2.

One of the objectives here is to determine how weak the stratification outside the primary wave guide must be in order for long, nonlinear waves with nearly zero frequency to be ducted along the wave guide. We know that, on a linear basis, waves with frequency ω cannot propagate in regions where the Brunt–Väisälä frequency is less than ω. However, in the case of nonlinear waves, we expect that this condition will depend in some way upon the wave amplitude.

(*a*) *The inner solution.* The appropriate slow space and time scales in the present case are

$$\xi = \epsilon x, \quad \tau = \epsilon^2 t, \tag{2.11}$$

and these are consistent with the evolution equation (1.2). Introducing these 'slow' variables and expanding the dependent variables in the manner

$$\psi = A(\xi,\tau)\,\phi(z) + \epsilon\psi^{(2)} + \dots, \tag{2.12a}$$

$$\sigma = -A\frac{N^2\phi}{U-c} + \epsilon\sigma^{(2)} + \dots, \tag{2.12b}$$

the same eigenvalue equation as in (2.6) is obtained except that the boundary conditions are modified to

$$\phi(0) = 0, \quad \lim_{z\to\infty}\phi(z) = 0. \tag{2.13}$$

Clearly, there are no non-trivial solutions of (2.6) satisfying these conditions when $U'', N^2 \to 0$ as $z \to \infty$, and, hence, the flow outside the wave-guide region must be considered separately (rescaled) and then matched to the (inner) solution of (2.6) valid within the wave guide. The necessity of the inner and outer matching is clear from the original work of Benjamin (1967) and Davis & Acrivos (1967). However, before moving on to consider that aspect of the analysis in the present context, we write the second-order equation in the inner region

$$\partial_\xi\left\{\partial_{zz}^2 - \frac{U''}{U-c} + \frac{N^2}{(U-c)^2}\right\}\psi^{(2)} = A_\tau \frac{2N^2-(U-c)\,U''}{(U-c)^3}\phi + AA_\xi[U'''(U-c)^2 - U'U''(U-c) - 2(U-c)\,(N^2)' + 3U'N^2]\frac{\phi^2}{(U-c)^4}. \tag{2.14}$$

A separable solution for $\psi^{(2)}$ is possible having the form

$$\psi^{(2)} = \mathscr{D}(A)f(z) + \tfrac{1}{2}A^2 g(z), \tag{2.15}$$

with $A(\xi, \tau)$ satisfying the evolution equation

$$A_\tau + \gamma A A_\xi + \delta(\mathscr{D}(A))_\xi = O(\epsilon). \tag{2.16}$$

Substituting (2.15) and (2.16) into (2.14) and invoking solvability yields, for non-critical-layer modes,

$$\lim_{z\to\infty}\{\phi f' - \phi' f\} = -\delta\int_0^\infty \frac{2N^2 - U''(U-c)}{(U-c)^3}\phi^2\,dz, \tag{2.17}$$

and

$$\lim_{z\to\infty}\{\phi g' - \phi' g\} = \int_0^\infty \frac{\phi^3}{(U-c)^4}[U'''(U-c)^2 - U''U'(U-c) - 2(U-c)\,(N^2)' + 3U'N^2]\,dz - \gamma\int_0^\infty \frac{2N^2 - U''(U-c)}{(U-c)^3}\phi^2\,dz. \tag{2.18}$$

As noted earlier, certain modifications are required when a critical layer exists. The left-hand sides of the last two equations and also the form of the unknown operator $\mathscr{D}$ must be determined by matching the above solutions of the inner problem to the outer solution obtained in the next section. The quantity $\mathscr{D}(A)$ is related to the first term in the long-wave limit of the dispersion relation, which, in turn, depends on the nature of the outer flow. When the fluid is homogeneous outside the thermoclinic wave guide, we know that $\mathscr{D}(A)$ is the first derivative with respect to ξ of the Hilbert transform of A (cf. Benjamin 1967; Ono 1975).

(*b*) *The outer solution.* The appropriate vertical length scale in the outer flow is no longer L, but the wavelength of the long wave propagating in the main thermocline. Hence, we define the stretched vertical co-ordinate

$$\zeta = \epsilon z. \tag{2.19}$$

The scales in x and z are now of the same order, which must be the case for both terms of the Laplacian in the vorticity equation (2.3) to be of equal importance, and a decaying solution as $\zeta \to \infty$ can be obtained. Then, using this scaling and the fact that ψ is still of order unity for matching to the inner solution, we must insist that the perturbation buoyancy $\sigma \leqslant O(\epsilon^2)$ in the outer region. This result, when substituted into equation (2.2), leads to the restriction that $N^2(z \to \infty) \leqslant O(\epsilon^2)$. Hence we find

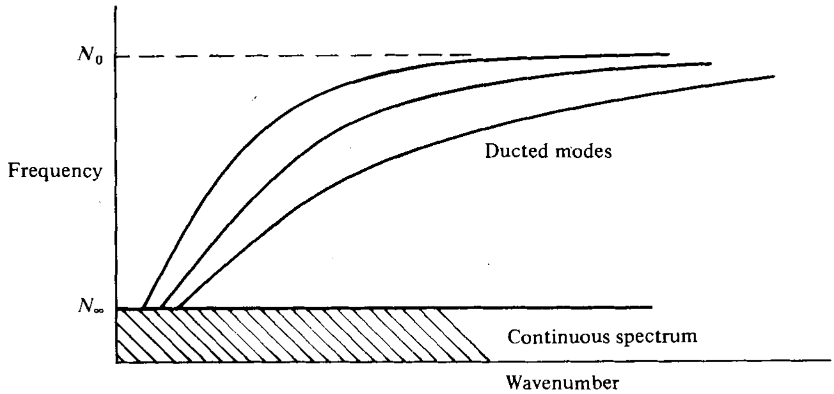

FIGURE 2. A schematic dispersion diagram for thermoclinic wave guides like those depicted in figure 1.

that the requirement for long waves to be ducted along an internal wave guide with characteristic frequency N_0 surrounded by an unbounded domain with characteristic frequency N_∞ is

$$a/L \gtrsim O(N_\infty/N_0), \tag{2.20}$$

where a is the wave amplitude. This condition is illustrated schematically in figure 2, where a composite dispersion diagram is included. The ducted wave modes can exhibit weakly nonlinear, long-wave behaviour (i.e. KdV-type motions) only if the amplitude is large enough relative to the ambient environment.

To analyse the outer flow we take

$$\lim_{z\to\infty} N(z) = \epsilon\mathcal{N}_\infty, \quad \mathcal{N}_\infty = O(1), \tag{2.21}$$

and write the following asymptotic expansions for the dependent variables

$$\psi_{\text{outer}} = \tilde{\psi}^{(1)}(\xi, \zeta, \tau) + \epsilon\tilde{\psi}^{(2)} + \ldots, \tag{2.22}$$

$$\sigma_{\text{outer}} = \epsilon^2\{\tilde{\sigma}^{(1)}(\xi, \zeta, \tau) + \epsilon\tilde{\sigma}^{(2)} + \ldots\}. \tag{2.23}$$

The leading-order problem can be expressed as

$$\{\partial^2_{\xi\xi} + \partial^2_{\zeta\zeta} + \alpha^2\}\,\tilde{\psi}^{(1)} = 0, \quad \alpha = \frac{\mathcal{N}_\infty}{|U_\infty - c|} = \text{constant},$$
$$\tilde{\psi}^{(1)}(\xi, \zeta = 0, \tau) = \mathscr{A}(\xi, \tau) = \lim_{z\to\infty} A\phi(z), \tag{2.24}$$

plus a radiation condition such that $\tilde{\psi}^{(1)}$ vanishes as $\zeta \to \infty$ and the solution is composed only of waves with a group velocity directed away from the main thermocline. At next order the field equation is

$$\{\partial^2_{\xi\xi} + \partial^2_{\zeta\zeta} + \alpha^2\}\,\tilde{\psi}^{(2)} = \frac{2\alpha^2}{U_\infty - c}\tilde{\psi}^{(1)}_\tau, \tag{2.25}$$

and the boundary condition at $\zeta = 0$ must be obtained from the higher-order terms in the inner solution. Since we are primarily interested in the leading-order terms in the amplitude evolution equation, we focus on the solution to (2.24).

The problem defined by equation (2.24) is a classical one in the theory of mountain lee waves in a uniform stratified flow (cf. Queney *et al.* 1960; or Miles 1968). The important difference in the present context is that the 'mountain shape' is determined by matching the inner and outer solutions, and it may also depend (slowly) on time. For this reason we sketch briefly the solution for $\tilde{\psi}^{(1)}$ and demonstrate the matching.

The solution is most readily achieved by Fourier methods. Defining the transform

$$\hat{\psi}^{(1)}(k,\zeta,\tau) = \int_{-\infty}^{\infty} \tilde{\psi}^{(1)}(\xi,\zeta,\tau)\, e^{-ik\xi}\, d\xi,$$

$$\tilde{\psi}^{(1)}(\xi,\zeta,\tau) = \frac{1}{2\pi}\int_{-\infty}^{\infty} \hat{\psi}^{(1)}\, e^{ik\xi}\, dk, \tag{2.26}$$

the solution $\hat{\psi}^{(1)}$ satisfying the radiation condition and the boundary condition for $c < U_\infty$ is

$$\hat{\psi}^{(1)}(k,\zeta,\tau) = \hat{\mathscr{A}}(k,\tau)\begin{cases}\exp[-\zeta(k^2-\alpha^2)^{\frac{1}{2}}], & |k| > \alpha,\\ \exp[i\zeta(\alpha^2-k^2)^{\frac{1}{2}}], & 0 < k < \alpha,\\ \exp[-i\zeta(\alpha^2-k^2)^{\frac{1}{2}}], & -\alpha < k < 0.\end{cases} \tag{2.27}$$

The opposite choice of signs in the exponent must be taken when $c > U_\infty$ for the solution in the range $-\alpha < k < \alpha$. This is the crucial step and corresponds precisely to the result obtained in Lyra (1943). Taking the inverse transform and expanding the solution for $\zeta \downarrow 0$, we obtain the matching condition

$$\lim_{\zeta\to 0}\tilde{\psi}^{(1)} = \mathscr{A}(\xi,\tau) - \frac{\alpha\zeta}{2}\, {}^{*}\!\!\int_{-\infty}^{\infty}\left\{\frac{Y_1(\alpha|\xi-\xi'|)}{|\xi-\xi'|} + \operatorname{sgn}(U_\infty - c)\frac{\mathscr{H}_1(\alpha|\xi-\xi'|)}{\xi-\xi'}\right\}\mathscr{A}(\xi',\tau)\, d\xi'$$
$$-\tfrac{1}{2}\zeta^2(\mathscr{A}_{\xi\xi}+\alpha^2\mathscr{A}) + O(\zeta^3), \tag{2.28}$$

where ${}^{*}\!\!\int$ denotes the Hadamard finite part of the integral (cf. Hadamard 1923). The function $Y_1(x)$ is the Bessel function of the second kind of order 1 and $\mathscr{H}_1(x)$ is the Struve function of order 1 (cf. Abramowitz & Stegun 1967). The latter term describes the energy loss or wave drag resulting from the fact that the ambient medium can support internal waves. Its magnitude is proportional to α and, hence, vanishes when the stratification in the outer environment tends to zero. The first term in the integrand describes the 'potential-like' motion in the outer flow and is singular. However, since the dominant contribution will come from the neighbourhood of the singularity, we can write

$$\frac{\alpha}{2}\, {}^{*}\!\!\int_{-\infty}^{\infty}\frac{Y_1(\alpha|\xi-\xi'|)}{|\xi-\xi'|}\mathscr{A}(\xi',\tau)\, d\xi' \simeq \frac{\partial}{\partial\xi}\left\{\frac{1}{\pi}\,⨍_{-\infty}^{\infty}\frac{\mathscr{A}(\xi',\tau)}{\xi-\xi'}\, d\xi'\right\}. \tag{2.29}$$

The right-hand side is identical with that obtained when the fluid outside the wave guide is homogeneous. The error involved in the approximation (2.29) is $O(\alpha)$ for weak stratification in the outer region. This approximate relation is used exclusively in what follows.

The evolution equation (2.16) can now be determined uniquely using the result given in (2.28). Choosing the following normalization for the leading-order eigenfunction

$$\lim_{z\to\infty}\phi'(z) = 0, \quad \lim_{z\to\infty}\phi(z) = 1, \tag{2.30}$$

the matching with the outer flow yields

$$\mathscr{A}(\xi,\tau) = A(\xi,\tau), \tag{2.31a}$$

$$\lim_{z\to\infty} f'(z) = -1, \tag{2.31b}$$

$$\lim_{z\to\infty} g(z) = 0, \tag{2.31c}$$

$$\mathscr{D}(A) = \frac{\partial}{\partial \xi}\left\{\frac{1}{\pi} \int_{-\infty}^{\infty} \frac{A(\xi',\tau)}{\xi-\xi'}\,d\xi'\right\} + \operatorname{sgn}(U_\infty - c)\frac{\alpha}{2}\int_{-\infty}^{\infty} \frac{\mathscr{K}_1(\alpha|\xi-\xi'|)}{\xi-\xi'} A(\xi',\tau)\,d\xi'. \tag{2.31d}$$

The evolution equation (2.16) can then be written as

$$A_\tau + \gamma A A_\xi + \delta \frac{\partial^2}{\partial \xi^2}\left\{\frac{1}{\pi}\int_{-\infty}^{\infty} \frac{A(\xi',\tau)}{\xi-\xi'}\,d\xi'\right\} = -\frac{\alpha\delta}{2}\operatorname{sgn}(U_\infty - c)\frac{\partial}{\partial \xi}\int_{-\infty}^{\infty} \frac{\mathscr{K}_1(\alpha|\xi-\xi'|)}{\xi-\xi'} A(\xi',\tau)\,d\xi', \tag{2.32}$$

with the coefficients δ and γ defined by

$$\delta^{-1} = \int_0^\infty \frac{\phi^2}{(U-c)^3}\{2N^2 - U''(U-c)\}\,dz, \tag{2.33a}$$

$$\gamma = \delta \int_0^\infty \frac{\phi^3}{(U-c)^4}\{U'''(U-c)^2 - U''U'(U-c) - 2(U-c)(N^2)' + 3U'N^2\}\,dz. \tag{2.33b}$$

Explicit evaluation of the coefficients for specific flow configurations together with further discussion of the evolution equation is deferred to later sections.

2.3. *Singular modes*

As noted earlier, long-wave solutions with critical layers are possible provided that nonlinearity rather than dissipation is the dominant effect there. In such cases, the integrals in (2.10) and (2.33) do not exist and a different solvability condition must be employed. The procedure will be demonstrated with specific examples in § 3. This section, however, deals with the nonlinear equations that apply in the critical layer itself. Only an outline is given because it develops that the equations and solution procedure are practically identical to that given by Maslowe (1972).

For the purposes of the present paper the principal result we require from the nonlinear critical-layer theory is that the eigensolutions behave as $|z-z_c|^{\frac{1}{2}\pm i\mu}$ on either side of the critical point. In the terminology of stability theory, there is no phase change, i.e. the constants multiplying the Frobenius expansions are the same on both sides of z_c. A streamline pattern that is symmetrical about z_c in the critical layer is compatible with the above requirement. At this point, some readers may wish to proceed directly to § 3. However, for the interest of those familiar with the nonlinear critical-layer theory the modifications that take place in the long-wave limit are indicated immediately below.

To reiterate a now well-known result, nonlinearity dominates in the critical layer when the parameter $\lambda \ll 1$, where λ is the cube of the ratio of the diffusive to the nonlinear boundary-layer thickness. For the KdV case $\lambda = (R\epsilon^{\frac{5}{2}})^{-1}$, R being the Reynolds number, whereas in the deep-water limit $\lambda = (R\epsilon^3)^{-1}$. The appropriate critical-layer variables for a nonlinear balance are

$$z - z_c = \epsilon^{\frac{2}{3}} Z, \quad \Psi = \epsilon^{\frac{4}{3}}\Phi(\xi, Z, \tau),$$

and

$$\rho_{\text{total}} - \rho_s(z_c) = \rho_0 \epsilon^{\frac{2}{3}}\Theta(\xi, Z, \tau), \tag{2.34}$$

where Ψ includes the mean flow in a frame of reference moving with the wave speed. In terms of these variables, the vorticity and temperature equations in the critical layer become

$$\{\epsilon^{\frac{1}{3}}\partial_\tau + \Phi_Z\partial_\xi - \Phi_\xi\partial_Z\}\Phi_{ZZ} + J_c\Theta_\xi = \lambda\Phi_{ZZZZ} \tag{2.35}$$

and

$$\{\epsilon^{\frac{1}{3}}\partial_\tau + \Phi_Z\partial_\xi - \Phi_\xi\partial_Z\}\Theta = \frac{\lambda}{Pr}\Theta_{ZZ}, \tag{2.36}$$

where Pr and J_c are, respectively, the Prandtl number and Richardson number at the critical point and higher-order terms have been omitted.

Neglecting the λ term, at least initially, it is clear that the quantities Φ and Θ should be expanded in powers of $\epsilon^{\frac{1}{3}}$. In order to determine the basic flow structure, only the solution at lowest order is required. Thus τ does not appear explicitly to this order and we obtain from (2.36) and (2.35), respectively,

$$\Theta^{(0)} = F(\Phi^{(0)}, \tau) \quad \text{and} \quad \Phi^{(0)}_{ZZ} = J_c Z F_{\Phi^{(0)}} + G(\Phi^{(0)}, \tau). \tag{2.37}$$

The functions F and G are arbitrary aside from the asymptotic conditions

$$F \sim (2\Phi^{(0)})^{\frac{1}{2}} \quad \text{and} \quad G \sim 1 - J_c \quad \text{as} \quad \Phi^{(0)} \to \infty. \tag{2.38}$$

These quantities can be fixed by imposing secularity conditions upon the $O(\lambda)$ perturbations to $\Theta^{(0)}$ and $\Phi^{(0)}$. However, our goal here is primarily to compute streamline patterns outside the dividing streamline in the critical layer. It was observed in Maslowe (1972) that for this purpose it is sufficient simply to set F and G to their asymptotic values. Note that (2.37) is essentially an ordinary differential equation expressing $\Phi^{(0)}$ as a function of Z. The dependence on the other variables appears only in the initial and boundary conditions; thus the streamline pattern can be established by repeatedly solving (2.37) for various values of the parameters ξ and τ.

3. The eigenvalue problem

In this section we present solutions of the eigenvalue problem (2.6) for several flow configurations and the evaluation of the respective coefficients in the evolution equations (1.1) and (1.2) for some of these flows. Both critical-layer (singular) modes and non-critical-layer (regular) modes are discussed.

The general flow configuration we consider is depicted schematically in figure 3. This particular model was chosen because it permits explicit analytical results and the use of broken-line profiles to approximate smooth flows is reasonable in the long-wave limit. Using the half-width L of the shear layer as the length scale and U_0 as the velocity scale, the eigenvalue equation within the shear layer is

$$\phi'' + \frac{J}{(z-c)^2}\phi = 0, \quad -1 < z < 1, \tag{3.1}$$

where $J = N_0^2/(U')^2$ is the (constant) Richardson number. We are interested principally in the linearly stable case when $J > \frac{1}{4}$ and the solution, both for regular and singular modes, can be written as

$$\phi = |z-c|^{\frac{1}{2}}\cos(\mu \ln|z-c| - \Delta), \tag{3.2}$$

where $\mu = (J-\frac{1}{4})^{\frac{1}{2}}$ and Δ is an arbitrary phase constant determined by the interface matching conditions. In the regions of homogeneous fluid above and below the shear

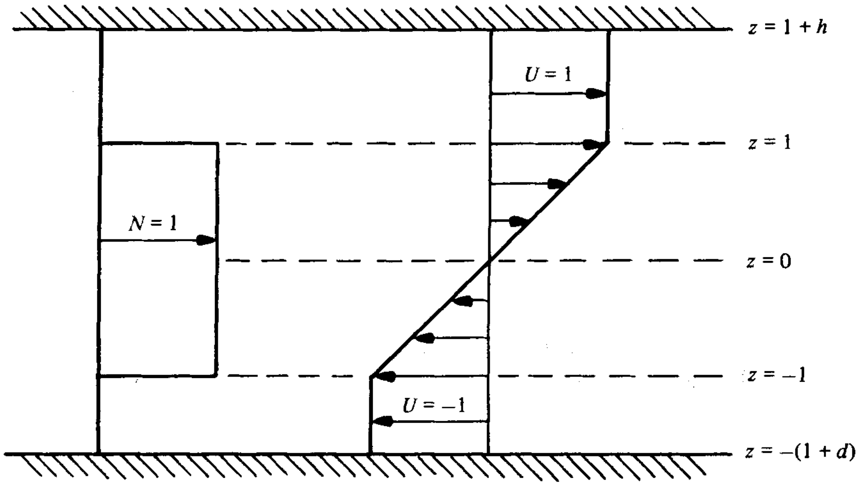

FIGURE 3. Flow model of the eigenvalue problem.

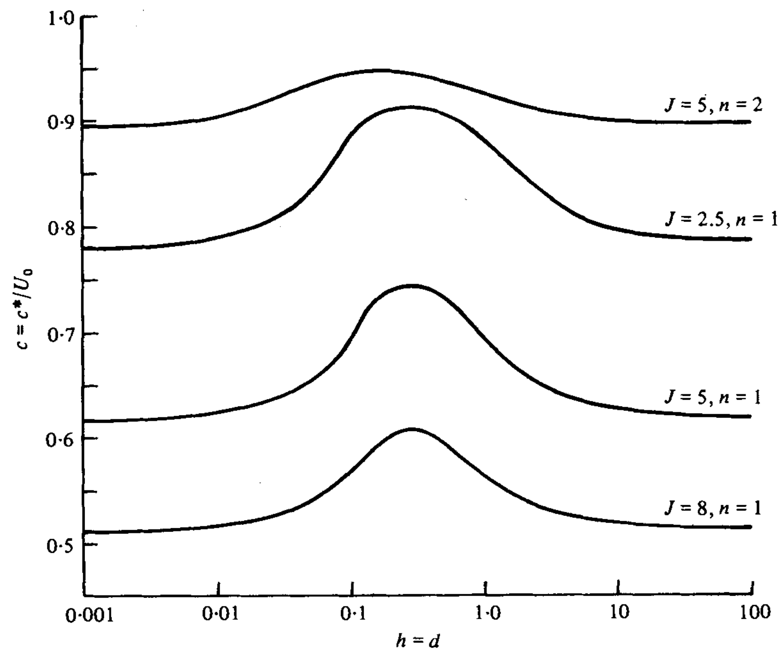

FIGURE 4. The long-wave phase speed as a function of boundary position for symmetrically located boundaries.

layer, the solution for arbitrary wavenumber k which satisfies the boundary conditions is

$$\phi = B_+ \sinh k(z-1-h), \quad 1 < z < 1+h, \tag{3.3a}$$

and

$$\phi = B_- \sinh k(z+1+d), \quad -(1+d) < z < -1. \tag{3.3b}$$

Of course, we have in mind the limit $k \downarrow 0$ which has already been imposed in (3.1), but the above form is useful in determining the dispersive corrections arising from the

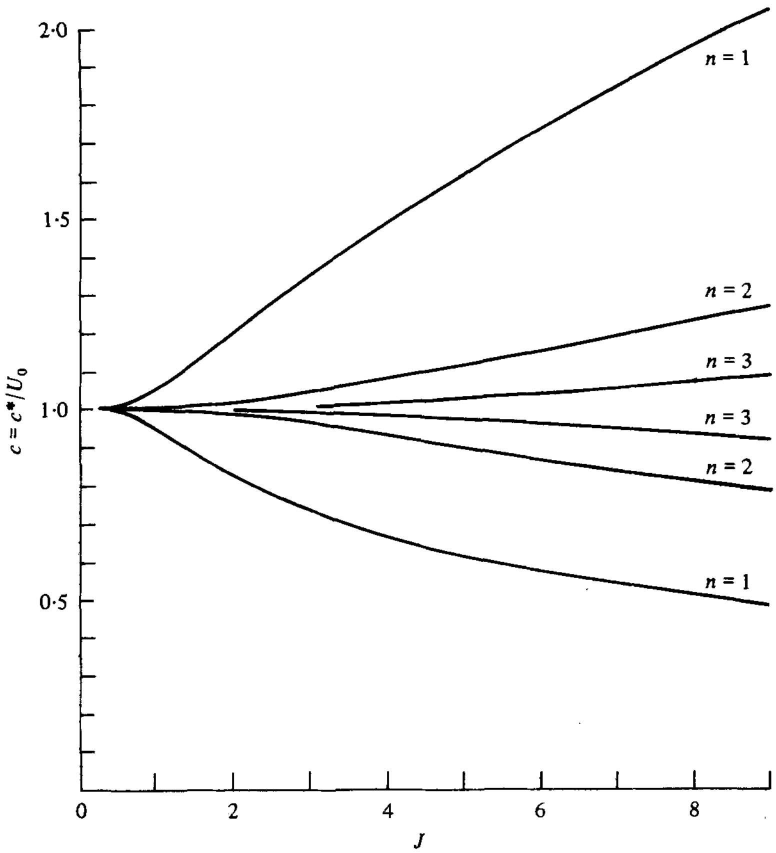

FIGURE 5. Eigenspeeds for long waves either in stratified Couette flow ($d = h = 0$) or an unbounded stratified shear flow ($d = h = \infty$).

presence of uniform flow regions adjacent to the shear layer. Invoking the kinematic condition (continuity of ϕ) and the dynamic condition (matching of the pressures)

$$[\![\phi']\!] = \frac{\phi}{z-c}[\![U']\!], \tag{3.4}$$

at the interfaces $z = \pm 1$, where $[\![...]\!]$ denotes the difference in the bracketed quantity evaluated immediately above and below the interface, we obtain the eigenvalue condition

$$\tan\left(\mu \ln\left|\frac{1+c}{1-c}\right|\right) = \frac{\mu\{h(1+c)-d(1-c)\}}{(1-c^2)-\frac{1}{2}d(1-c)-\frac{1}{2}h(1+c)+hd(\mu^2+\frac{1}{4})}. \tag{3.5}$$

Certain limits of this expression are interesting to consider. First, taking either the limit $d = h = 0$ (Couette flow) or $d = h \to \infty$, we obtain the same eigenvalue condition, namely

$$c = \pm \tanh\left(\frac{n\pi}{2\mu}\right), \quad n = 0, 1, 2, ..., \tag{3.6}$$

for critical-layer modes and

$$c = \pm \coth\left(\frac{n\pi}{2\mu}\right), \quad n = 1, 2, 3, ..., \tag{3.7}$$

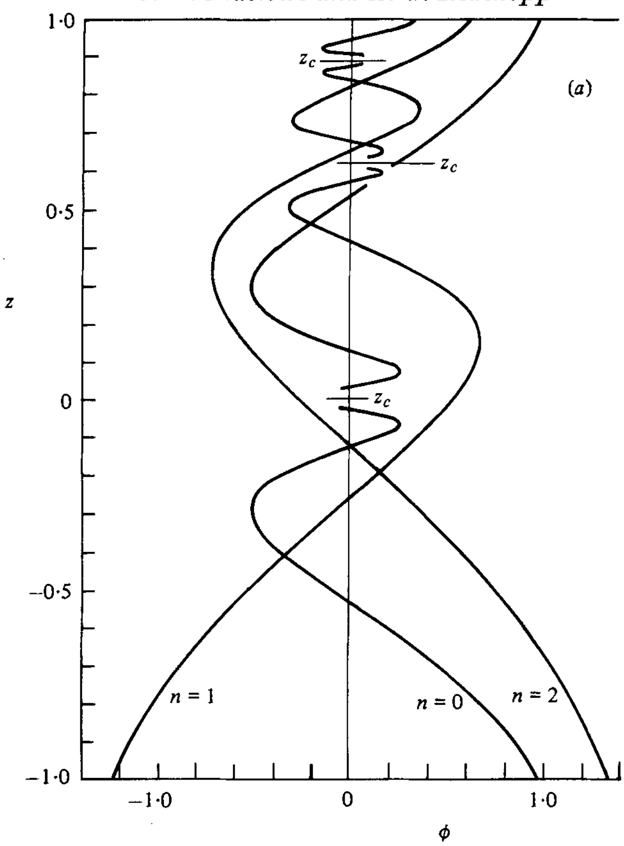

FIGURE 6 (a). For legend see page 336.

for non-critical layer (internal wave) modes. The latter relation for the case with $d = h = 0$ was first given by Hoiland (1953), but the singular modes have not been considered before. The stationary ($n = 0$) singular neutral mode in (3.6) was found numerically by Maslowe (1973), but the propagating modes ($0 < |c| < 1$), which were conjectured to exist in that paper, are exhibited here explicitly. That the eigenvalue relation is the same for both depth limits is unexpected. However, this is due to the fact that the pressure is constant on the boundary of the shear layer in the long-wave limit for both cases. Numerical calculations of the eigenvalue c as a function of the boundary position for the symmetric case with $d = h$ is shown in figure 4 for several Richardson numbers. The waves first speed up as the boundaries are removed and then slow down again as the boundaries become one thermocline thickness or more distant from the wave guide. Computations of (3.6) and (3.7) for different mode numbers n are presented in figure 5. As n increases, the modes become more packed into the corners of the shear layer. Some typical eigenfunctions are presented in figure 6.

Another useful limit of (3.5) is to take $d = 0$ and $h \to \infty$, in that order. Then, if one makes a Galilean transformation and rescales the shear-layer thickness to correspond to the configuration shown in figure 7, the eigenvalue condition takes the form

$$c = \left\{1 + \exp\left[\frac{1}{\mu}\tan^{-1}(2\mu) - \frac{n\pi}{\mu}\right]\right\}^{-1}, \quad n = 0, \pm 1, \pm 2, \ldots, \tag{3.8}$$

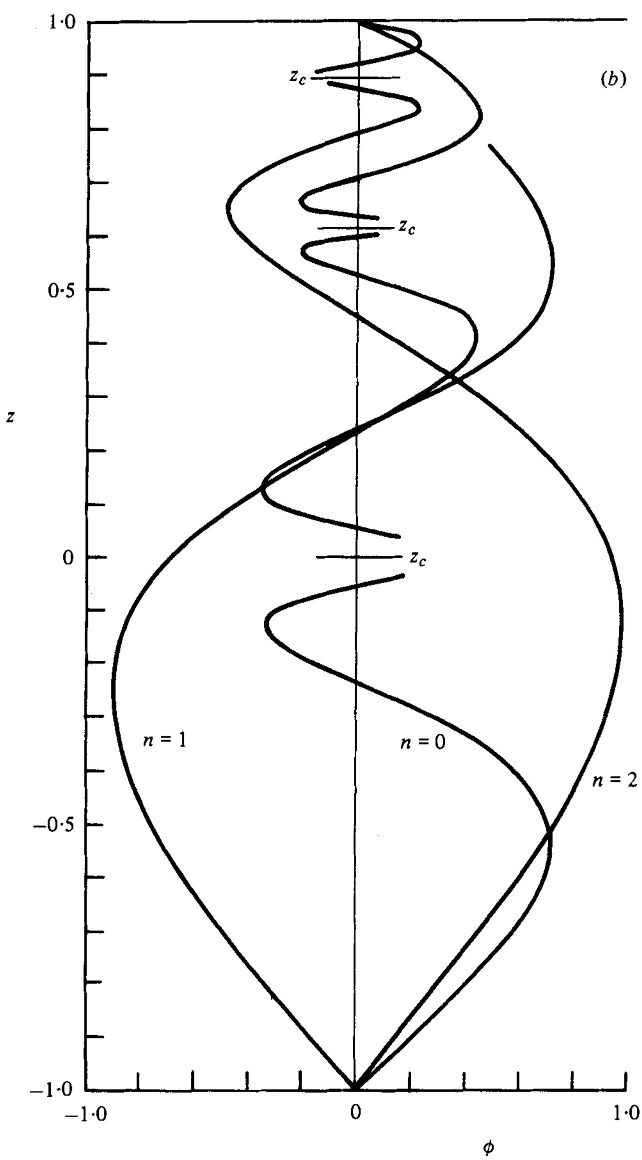

FIGURE 6(b). For legend see page 336.

for critical-layer modes and

$$c = \left\{1 - \exp\left[\frac{1}{\mu}\tan^{-1}(2\mu) - \frac{n\pi}{\mu}\right]\right\}^{-1}, \quad n = 0, \pm 1, \pm 2, \ldots, \tag{3.9}$$

for (non-singular) internal wave modes.

Another limit process of some interest is the behaviour of the modes for large Richardson numbers. For singular modes the long-wave phase speed varies as $nJ^{-\frac{1}{2}}$. For the internal wave modes described by (3.7), the limit $J \gg 1$ or, more appropriately, the

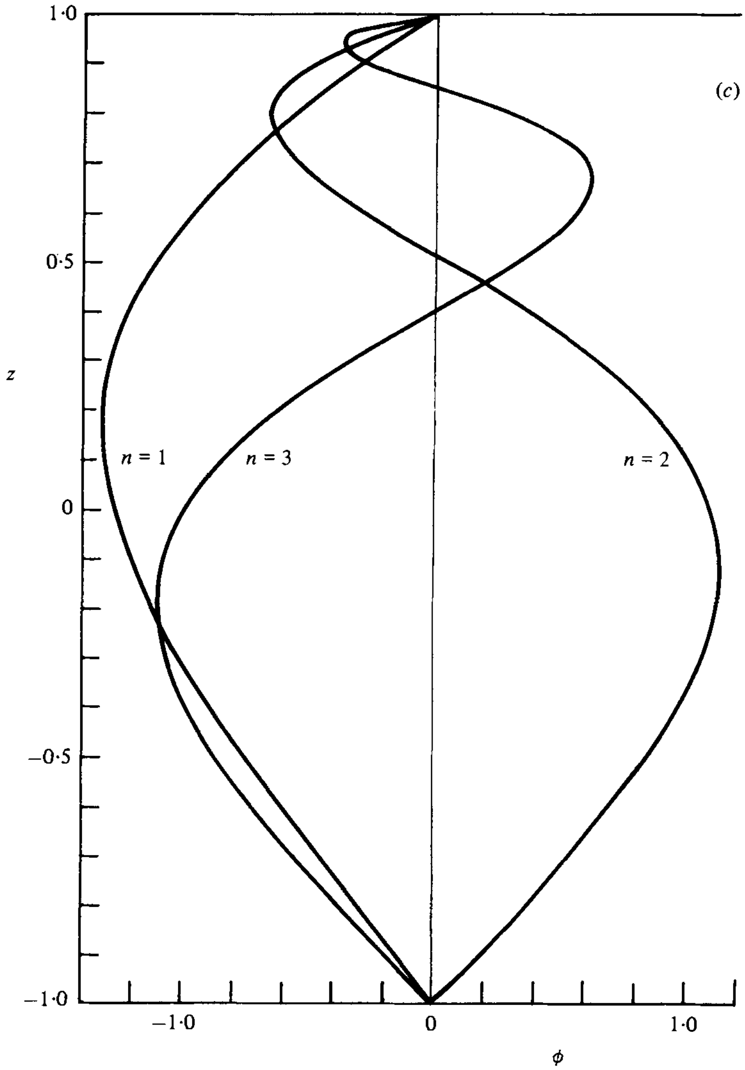

FIGURE 6. Typical eigenfunctions for: (a) singular modes in an unbounded shear flow ($d = h = \infty$, $J = 5$); (b) singular modes in Couette flow ($d = h = 0$, $J = 5$); and (c) internal wave modes in Couette flow ($J = 8$). The value z_c denotes the location of the critical level.

limit $F \downarrow 0$ when using the scaling in (2.4), yields

$$c^* = \pm\frac{N_0 b}{n\pi}\left\{1+\frac{(n\pi)^2}{12J}+\ldots\right\}, \quad 1 \leqslant n < \infty, \tag{3.10}$$

and in (3.9) it yields

$$c^* = \frac{N_0 b}{(n-\frac{1}{2})\pi}\left\{1+\frac{(n-\frac{1}{2})\pi}{2J^{\frac{1}{2}}}+\ldots\right\}, \quad 1 \leqslant |n| < \infty. \tag{3.11}$$

In the last two expressions the variable c^* is used to denote the dimensional phase velocity and b is the thickness of the stratified layer with constant Brunt–Väisälä frequency N_0. For the unbounded case ($d = h \to \infty$), there is an additional mode

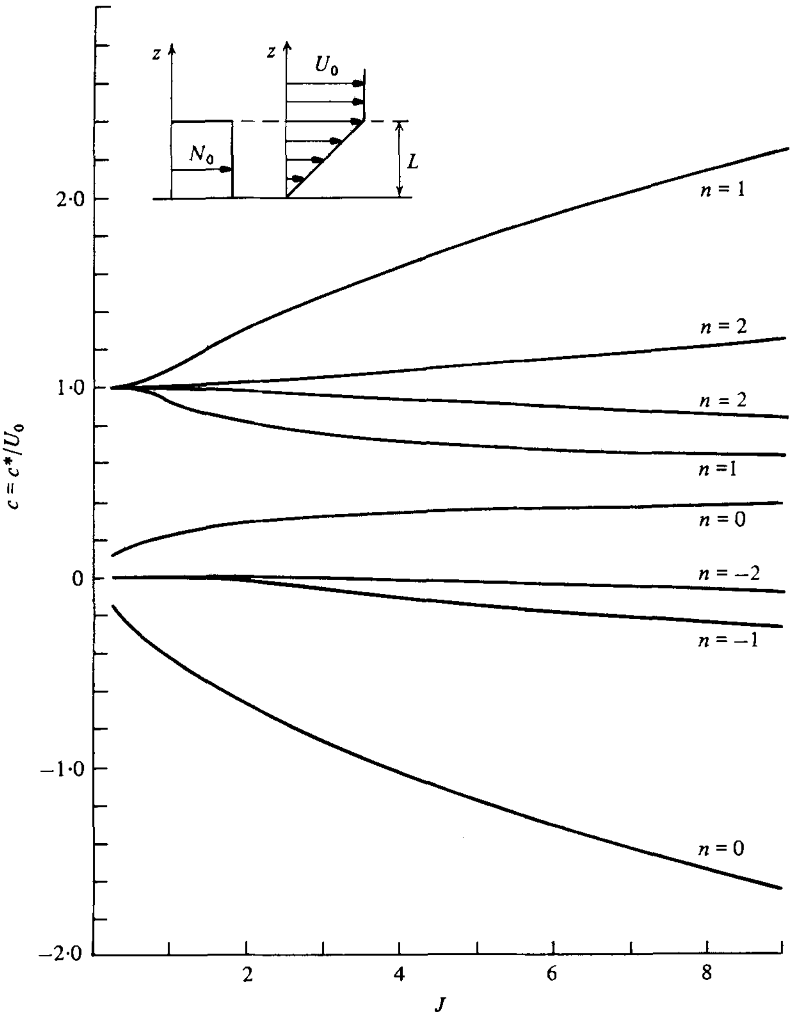

FIGURE 7. Eigenspeeds for a boundary-layer flow model.

corresponding to the interfacial (gravity) wave mode, but it has an unbounded long-wave phase velocity and is excluded from the analysis here.

3.1. *KdV coefficients*

We present here the calculation of the coefficients α and β (cf. equations (1.1) and (2.10)) appearing in the KdV equation for the special case of stratified Couette flow (viz. figure 3, $d = h = 0$). The long-wave phase speed for these modes is given by (3.6) and (3.7) with the eigenfunction (3.2). Because the integrals in (2.10) do not exist for the singular modes, we evaluate the coefficients by solving directly equations (2.8) and (2.9) for the second-order modal functions, invoking the result of the non-linear-critical-layer analysis that there is no phase change across the critical layer even to this order, and then apply the homogeneous boundary conditions at $z = \pm 1$.

The general solutions of equations (2.8) and (2.9) are

$$\phi_d^{(2)}(z) = a_d^{(2)}|z-c|^{\frac{1}{2}}\cos(\mu\ln|z-c|-\Delta_d^{(2)}) - \frac{|z-c|^{\frac{5}{2}}}{4J+3}(\mu\sin(\mu\ln|z-c|-\Delta)+\cos(\mu\ln|z-c|-\Delta)) + \beta\left\{\frac{\operatorname{sgn}(z-c)}{|z-c|^{\frac{1}{2}}}(\mu\sin(\mu\ln|z-c|-\Delta)-\tfrac{1}{2}\cos(\mu\ln|z-c|-\Delta))\right\} \quad (3.12)$$

and

$$\phi_n^{(2)}(z) = a_n^{(2)}|z-c|^{\frac{1}{2}}\cos(\mu\ln|z-c|-\Delta_n^{(2)}) + \alpha\frac{\operatorname{sgn}(z-c)}{|z-c|^{\frac{1}{2}}}(\mu\sin(\mu\ln|z-c|-\Delta)-\tfrac{1}{2}\cos(\mu\ln|z-c|-\Delta)) + \left\{\frac{3J}{2(J+2)}|z-c|^{-1}+\frac{|z-c|^{-1}}{J+2}\left[\frac{1-J}{2}\cos 2(\mu\ln|z-c|-\Delta) - \mu\sin 2(\mu\ln|z-c|-\Delta)\right]\right\}. \quad (3.13)$$

The first terms in each expression are the homogeneous solutions with amplitudes $a^{(2)}$ and phases $\Delta^{(2)}$. The constant Δ is already determined by the leading-order solution to be

$$\Delta = \frac{\mu}{2}\ln|1-c^2| - \frac{(n+1)\pi}{2}. \quad (3.14)$$

Then, applying the boundary conditions, we obtain the results

$$\left.\begin{aligned}\beta &= -\frac{2c(1-c^2)}{4J+3},\\ \alpha &= \frac{\mu}{J+2}\,\frac{(1-c)^{\frac{3}{2}}-(-1)^n(1+c)^{\frac{3}{2}}}{(1-c^2)^{\frac{1}{2}}}\end{aligned}\right\} \quad (3.15)$$

for singular neutral modes $(-1 < c < 1)$. Observe that both coefficients vanish for the $n = 0$ mode, for which $c = 0$. That $\beta = 0$ for this mode reflects the fact that it is dispersionless and exists for all wavenumbers and $J > \frac{1}{4}$. It is surprising that the nonlinear terms are zero to this order also. As we demonstrate later, the same results are obtained for the unbounded case $d = h \to \infty$. However, any asymmetry in the boundary position $(d \neq h)$ will lead to non-zero values for α and β.

An important parameter which appears in the solitary-wave solution of (1.1), viz.

$$A(\xi,\tau) = \operatorname{sgn}(\alpha\beta)\operatorname{sech}^2\{\kappa(\xi-c^{(1)}\tau)\}, \quad (3.16)$$

is the wavenumber κ defined by

$$\kappa = \left|\frac{\alpha}{12\beta}\right|^{\frac{1}{2}} = \left|\frac{(4J+3)\mu}{24(J+2)}\,\frac{(1-c)^{\frac{3}{2}}-(-1)^n(1+c)^{\frac{3}{2}}}{c(1-c^2)^{\frac{3}{2}}}\right|^{\frac{1}{2}}. \quad (3.17)$$

As $J \downarrow \frac{1}{4}$, the phase speed behaves as $|c| \uparrow 1$ and κ is unbounded. The eigenfunction solution does not permit discussion of the point $J = \frac{1}{4}$, but the limit shows that the solitary wave for these singular modes gets progressively shorter as the linear stability limit is approached. As $J \to \infty$, κ is proportional to $J^{\frac{1}{2}}$ for odd n and is proportional to $J^{\frac{1}{4}}$ for even n. The wavenumber has a minimum at intermediate values of J. Hence, for a fixed wave amplitude and thermoclinic length scale, the solitary wavelength depends strongly on the Richardson number, especially for $\frac{1}{4} < J < 1$.

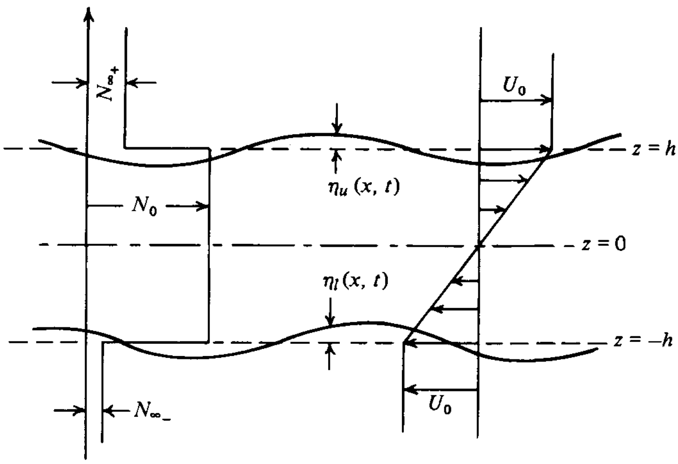

FIGURE 8. Flow model and notation for the unbounded shear flow with weak background stratification outside the main thermocline.

When $|c| > 1$ and $d = h = 0$, the corresponding values for the coefficients are

$$\beta = \frac{2c(c^2-1)}{4J+3},$$

$$\alpha = -\frac{\mu}{J+2} \frac{|1+c|^{\frac{3}{2}} - (-1)^n |1-c|^{\frac{3}{2}}}{(c^2-1)^{\frac{1}{2}}}, \tag{3.18}$$

where c is given by (3.7). The integrals in (2.10) are well-defined in this case and α and β can be evaluated directly, although the computation is lengthy.

3.2. *mdKdV coefficients*

The evaluation of the coefficients γ and δ in equation (1.2) for the flow model displayed in figure 3 requires a somewhat different analysis from that presented in § 2. This occurs because no intermediate overlap domain exists where both the inner and outer solutions have a common region of validity when the derivative of the eigenfunction is discontinuous at some interior point. Instead, the matching of the solutions must be accomplished at the interface locations $z = h + \eta_u(x,t)$ and $z = -h + \eta_l(x,t)$ (see figure 8), where η_u and η_l are the interface distortions at the upper and lower corners of the stratified shear layer, respectively. The matching conditions that must be applied at both interfaces are the kinematic condition

$$w = \frac{D\eta}{Dt} \tag{3.19}$$

and the condition that the total pressure is continuous across each interface

$$[\![p_{\text{total}}]\!] = 0. \tag{3.20}$$

The bracket symbol $[\![\ldots]\!]$ denotes the difference between the bracketed quantity evaluated immediately above and below a particular interface.

Referring to the flow configuration shown in figure 8, the undisturbed pressure field is given by

$$\frac{p_s(z)-p_s(0)}{\rho_0}+gz=\begin{cases}\frac{1}{2}N_{\infty+}^2(z-h)^2+N_0^2h(z-\frac{1}{2}h), & z>h,\\ \frac{1}{2}N_0^2z^2, & -h<z<h,\\ \frac{1}{2}N_{\infty-}^2(z+h)^2-N_0^2h(z+\frac{1}{2}h), & z<h.\end{cases} \tag{3.21}$$

Then, using the normalization discussed in § 2 and writing the pressure as

$$\frac{p_{\text{total}}}{\rho_0N_0^2h^2}=P_s(z)+\epsilon(p^{(1)}+\epsilon p^{(2)}+\dots), \tag{3.22}$$

for the inner region $(-1<z<1)$, and

$$\frac{p_{\text{total}}}{\rho_0N_0^2h^2}=P_s(z)+\epsilon^2(\tilde{p}^{(1)}+\epsilon\tilde{p}^{(2)}+\dots) \tag{3.23}$$

for the outer region $(|z|>l)$, we obtain the sequence of pressure-matching conditions

$$(p^{(1)}+\eta_u^{(1)}P_s')|_{z=1-}=(\eta_u^{(1)}P_s')|_{z=1+}, \tag{3.24a}$$

$$(p^{(2)}+\tfrac{1}{2}(\eta_u^{(1)})^2P_s''+\eta_u^{(2)}P_s'+\eta_u^{(1)}p^{(1)})|_{z=1-}=(\tilde{p}^{(1)}+\tfrac{1}{2}(\eta_u^{(1)})^2P_s''+\eta_u^{(2)}P_s')|_{z=1+}. \tag{3.24b}$$

Similar conditions apply at $z=-1$ and the interface displacements have been expanded as

$$\eta_i=h[\epsilon\eta_i^{(1)}+\epsilon^2\eta_i^{(2)}+\dots],\quad i=u,l. \tag{3.25}$$

The pressure terms for the inner layer are related to the stream function by

$$p^{(1)}=-(U-c)\psi_z^{(1)}+U'\psi^{(1)}=A(\xi,\tau)\{U'\phi-(U-c)\phi'\}, \tag{3.26a}$$

$$p^{(2)}=-(U-c)\psi_z^{(2)}+U'\psi^{(2)}-\tfrac{1}{2}A^2\{(\phi')^2-\phi\phi''\}-\phi'\int^\xi A_\tau\,d\xi, \tag{3.26b}$$

and, for the outer layer, we have the result

$$\left.\begin{aligned}\tilde{p}^{(1)}(z=\pm1)=\operatorname{sgn}z[U(\pm1)-c]\Bigg\{&\frac{\partial}{\partial\xi}\left[\frac{1}{\pi}\int_{-\infty}^{\infty}\frac{\mathscr{A}_\pm(\xi',\tau)}{\xi-\xi'}d\xi'\right]\\ &+\operatorname{sgn}[U(\pm1)-c]\frac{\alpha_\pm}{2}\int_{-\infty}^{\infty}\mathscr{A}_\pm(\xi',\tau)\frac{\mathscr{H}_1(\alpha_\pm|\xi-\xi'|)}{\xi-\xi'}d\xi'\Bigg\},\\ \alpha_\pm=\frac{\mathscr{N}_{\infty\pm}}{|U(\pm1)-c|}.\end{aligned}\right\} \tag{3.27}$$

Noting that P_s' is continuous across the interfaces, the first pressure matching condition yields

$$p^{(1)}(1)=p^{(1)}(-1)=0. \tag{3.28}$$

This is just the eigenvalue condition for c and shows that, to leading order, the pressure perturbation vanishes at the shear-layer edges. The first-order kinematic conditions lead to the relations

$$\mathscr{A}_\pm=\phi(\pm1)A(\xi,\tau),$$

and

$$\eta^{(1)}=\mp\frac{\phi(\pm1)}{[(U\pm1)-c]}A, \tag{3.29}$$

where the upper and lower signs apply for η_u and η_l, respectively.

To complete the derivation of the amplitude equation and the evaluation of the coefficients, we need the solution of $\psi^{(2)}$ from (2.14) to substitute into the second of the pressure matching conditions. It turns out that the separation invoked in (2.15) and (2.16) is too restrictive when the outer flows above and below the shear layer are not identical ($N_{\infty+} \neq N_{\infty-}$). Instead, we write the solution for $\psi^{(2)}$ in the form

$$\psi^{(2)} = \frac{A^2}{2}\phi_r^{(2)} + \left(\int^{\xi} A_\tau \, d\xi\right)\phi_t^{(2)} + \mathscr{T}(A)\,\phi_0^{(2)}, \tag{3.30}$$

where the last term is an arbitrary function of the amplitude A multiplied by the solution of the homogeneous equation. The functions $\phi_r^{(2)}$ and $\phi_t^{(2)}$ are just the appropriate particular solutions for the nonlinear and linear terms on the right-hand side of (2.14). The pressure matching condition then yields the two equations

$$\left.\begin{aligned} a_{1+}A_\tau + a_{2+}AA_\xi + a_{3+}\{\mathscr{T}(A)\}_\xi &= a_{4+}\frac{\partial I_+}{\partial \xi},\\ a_{1-}A_\tau + a_{2-}AA_\xi + a_{3-}\{\mathscr{T}(A)\}_\xi &= a_{4-}\frac{\partial I_-}{\partial \xi},\\ I_\pm = \frac{\partial}{\partial \xi}\left\{\frac{1}{\pi}\int_{-\infty}^{\infty}\frac{A(\xi',\tau)}{\xi-\xi'}\,d\xi'\right\} & \\ +\frac{\alpha_\pm}{2}\operatorname{sgn}[U(\pm 1)-c]\int_{-\infty}^{\infty} & A(\xi',\tau)\frac{\mathscr{H}_1(\alpha_\pm|\xi-\xi'|)}{\xi-\xi'}\,d\xi', \end{aligned}\right\} \tag{3.31}$$

where the coefficients, for the flow model depicted in figure 8, have the definitions

$$a_{1\pm} = \{-(U-c)\,\phi_t^{(2)\prime} + U'\phi_t^{(2)} - \phi'\}|_{z=\pm 1}, \tag{3.32a}$$

$$a_{2\pm} = \left\{-(U-c)\,\phi_r^{(2)\prime} + U'\phi_r^{(2)} - (\phi')^2 - 2\left(\frac{\phi}{U-c}\right)^2\right\}\Bigg|_{z=\pm 1}, \tag{3.32b}$$

$$a_{3\pm} = \{-(U-c)\,\phi_0^{(2)\prime} + U'\phi_0^{(2)}\}|_{z=\pm 1}, \tag{3.32c}$$

$$a_{4\pm} = \pm\{\phi(U-c)\}|_{z=\pm 1}. \tag{3.32d}$$

Compatibility requirements on the quantity $\mathscr{T}(A)$ in the two equations then yield the evolution equation

$$A_\tau + \gamma AA_\xi - \delta_+\frac{\partial I_+}{\partial \xi} - \delta_-\frac{\partial I_-}{\partial \xi} = 0, \tag{3.33}$$

and the coefficients have the values

$$\gamma = \frac{a_{2+}a_{3-} - a_{2-}a_{3+}}{a_{1+}a_{3-} - a_{1-}a_{3+}}, \tag{3.34a}$$

$$\delta_\pm = \pm\frac{a_{4\pm}a_{3\mp}}{a_{1+}a_{3-} - a_{1-}a_{3+}}. \tag{3.34b}$$

Based on the above results, we present values for γ and $\delta_\pm$ for four specific flow models. Model I (a) corresponds to the unbounded stratified shear flow shown in figure 8 and model I (b) corresponds to the semi-infinite configuration in which a solid boundary is placed at $z = 0$. Models II (a) and II (b) are similar but the shear is taken to be zero (i.e. $U_0 = 0$). For models I(a, b) the eigenfunction is given by (3.2) and the

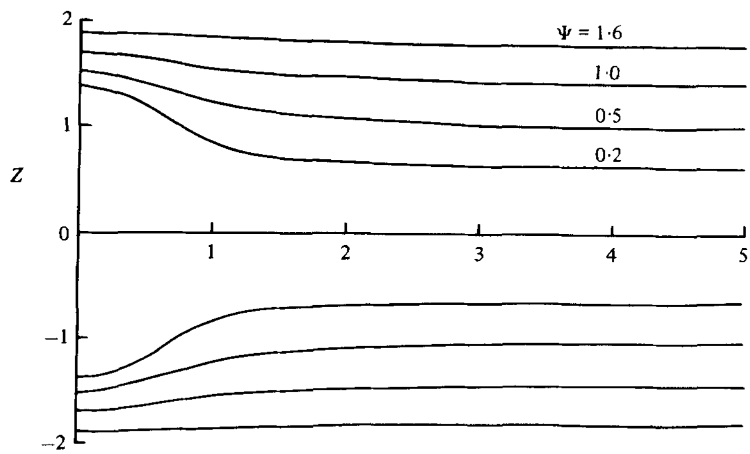

FIGURE 9. Outer streamline pattern for model I(*a*) with $J = 5$, $n = 1$ and $\epsilon = 0{\cdot}25$.

functions $\phi_t^{(2)}$ and $\phi_r^{(2)}$ are given by the last bracketed terms in equations (3.12) and (3.13), respectively. For model II(*a*), the appropriate solutions are

$$\left.\begin{aligned} \phi &= \sin\left(\frac{2n-1}{2}\pi z\right), \\ c &= \frac{2}{(2n-1)\pi}, \\ \phi_t^{(2)} &= \frac{z}{c^2}\cos\left(\frac{2n-1}{2}\pi z\right), \end{aligned}\right\} \quad n = 1, 2, \ldots, \tag{3.35}$$

for the odd modes and

$$\left.\begin{aligned} \phi &= \cos(n\pi z), \\ c &= \frac{1}{n\pi}, \\ \phi_t^{(2)} &= -\frac{z}{c^2}\sin(n\pi z), \end{aligned}\right\} \quad n = 1, 2, \ldots, \tag{3.36}$$

for the even modes. The function $\phi_r^{(2)}$ is identically zero for both the even and the odd modes of model II(*a*). This is expected from the earlier discussion following equation (2.10). Only the odd modes which automatically satisfy the required condition on a solid boundary at $z = 0$ are permissible for model II(*b*). Then, substituting these results into the coefficient expressions (3.32), we obtain the results shown in table 1 for γ and $\delta_\pm$. The stationary singular mode ($n = c = 0$) for model I(*a*) has $\gamma = 0$. Also, the dispersive terms in the evolution equation (3.33) will exactly cancel if the flows above and below the shear layers are identical (i.e. $N_{\infty+} = N_{\infty-}$). Under these conditions, this particular mode is dispersionless as explained earlier. The coefficients are non-zero for the remaining discrete set of modes for both models I(*a*, *b*). The coefficient γ of the nonlinear term vanishes identically for all even modes in model II(*a*). This occurs because of the symmetry of the eigenfunction and the flow configuration. A nonlinear dispersive balance can be achieved on a longer time scale $O(\epsilon^{-4})$ leading to an equation with cubic nonlinearity. The non-zero value of γ for the odd modes in the Boussinesq approximation results entirely from the nonlinear terms

Flow model	Eigenvalue relation	γ	δ_+	δ_-
I (a) singular modes	$c = \pm\tanh\left(\frac{n\pi}{2\mu}\right)$	$-\frac{\mu J^{\frac{1}{2}}}{J+2}\,\frac{(1+c^2)^{\frac{3}{2}}-(-1)^n(1-c)^{\frac{3}{2}}}{(1-c^2)^{\frac{1}{2}}}$	$-\frac{1}{2J}(1-c)(1-c^2)$	$\frac{1}{2J}(1+c)(1-c^2)$
I (a) internal wave modes	$c = \pm\coth\left(\frac{n\pi}{2\mu}\right)$	$\frac{\mu J^{\frac{1}{2}}}{J+2}\,\frac{\lvert 1+c\rvert^{\frac{3}{2}}-(-1)^n\lvert 1-c\rvert^{\frac{3}{2}}}{(c^2-1)^{\frac{1}{2}}}$	$\frac{1}{2J}(c-1)(c^2-1)$	$\frac{1}{2J}(1+c)(c^2-1)$
I (b) singular modes	Equation (3.8)	$-\frac{2\mu}{J+2}\,\frac{(-1)^n J^{\frac{1}{2}} c^{\frac{3}{2}}+(1-c)^{\frac{3}{2}}}{c^{\frac{1}{2}}(1-c)^{\frac{1}{2}}}$	$-\frac{1}{J}(1-c^2)$	0
I (b) internal wave modes	Equation (3.9)	$-\frac{2\mu}{J+2}\,\frac{(-1)^n J^{\frac{1}{2}}\lvert c\rvert^{\frac{3}{2}}+\lvert 1-c\rvert^{\frac{3}{2}}}{\lvert c(1-c)\rvert^{\frac{1}{2}}\{\lvert c\rvert\,\mathrm{sgn}\,(1-c)+\lvert 1-c\rvert\,\mathrm{sgn}\,c\}}$	$\frac{1}{J}\,\frac{\mathrm{sgn}\,(1-c)\,\lvert c\rvert(1-c)^2}{\lvert c\rvert\,\mathrm{sgn}\,(1-c)+\lvert 1-c\rvert\,\mathrm{sgn}\,c}$	0
II (a) odd modes	$c = \pm\frac{2}{(2n-1)\pi}$	$2(-1)^{n+1}$	$\frac{1}{2}c^3$	$-\frac{1}{2}c^3$
II (a) even modes	$c = \pm\frac{1}{n\pi}$	0	$\frac{1}{2}c^3$	$-\frac{1}{2}c^3$
II (b)	$c = \pm\frac{2}{(2n-1)\pi}$	$(-1)^{n+1}$	c^3	0

TABLE 1

in the interface matching condition (3.24*b*) where the gradient of the Brunt–Väisälä profile is non-zero (cf. equation (2.33*b*)). The solution for the first odd mode in model II (*a*) was given earlier by Davis & Acrivos (1967).

In figure 9 we present an example of the streamline pattern for a singular mode in the unbounded case (i.e. flow model I (*a*)). Only the outer structure is exhibited in the figure because the dividing streamline shape varies somewhat depending on the wave amplitude and the ambient Richardson number. This occurs because the vertical wavelength of the eigensolution (3.2) depends strongly on these parameters near the critical level. The eddy structure corresponding to the singular solutions presented here as well as the influence of finite Reynolds numbers on these patterns is deserving of further study.

4. The radiation damping of a solitary wave

We have shown that finite-amplitude long waves can be ducted along a thermoclinic wave guide providing the ambient environment above and below the wave guide is only weakly stratified. The weak stratification in the outer regions supports internal wave motion and, therefore, serves as an energy sink for waves propagating in the main thermocline. In this section we compute the damping rate resulting from this wave-drag mechanism and give the decay characteristics for a solitary wave.

The desired results can be derived most readily from the evolution equation (2.32). It is convenient for this purpose to rewrite the equation with the kernel of the integral operator replaced by its integral representation

$$A_\tau + \gamma A A_\xi + \delta \frac{\partial^2}{\partial \xi^2}\left\{\frac{1}{\pi}\int_{-\infty}^{\infty} \frac{A(\xi',\tau)}{\xi-\xi'}\,d\xi'\right\}$$
$$= -\delta\,\mathrm{sgn}\,(U_\infty - c)\int_{-\infty}^{\infty} A(\xi',\tau)\,d\xi'\left\{\frac{1}{\pi}\int_0^{\alpha} k(\alpha^2-k^2)^{\frac{1}{2}}\cos k(\xi-\xi')\,dk\right\}. \qquad (4.1)$$

The coefficient $\delta\,\mathrm{sgn}\,(U_\infty - c)$ is positive for all cases investigated here and must be so in general if the term on the right-hand side is to represent an energy loss. It is clear from (2.33*a*) that, in the absence of velocity shear, $\delta\,\mathrm{sgn}\,(U_\infty - c)$ is positive, but we have not been able to provide a general proof of this result. Suppose $A(\xi,\tau)$ corresponds to some localized wave packet. Then, after integrating the equation once with respect to the spatial co-ordinate ξ, one obtains

$$\frac{\partial}{\partial \tau}\langle A\rangle = \frac{\partial}{\partial \tau}\int_{-\infty}^{\infty} A(\xi,\tau)\,d\xi = 0. \qquad (4.2)$$

This relation shows that the volume of the packet is conserved. If the equation is first multiplied by A and then integrated, the energy decay law

$$\frac{\partial}{\partial t}\langle A^2\rangle = -\frac{2|\delta|}{\pi}\int_0^{\alpha} k(\alpha^2-k^2)^{\frac{1}{2}}\,|F(k,\tau)|^2\,dk, \qquad (4.3)$$

is obtained, where $F(k,\tau)$ is the Fourier transform of the wave profile

$$F(k,\tau) = \int_{-\infty}^{\infty} A(\xi,\tau)\,e^{ik\xi}\,dk.$$

This demonstrates that the term on the right-hand side of the evolution equation describes an energy loss and that the decay rate vanishes in the limit as the density stratification in the outer region approaches zero (i.e. $\alpha \to 0$). Corresponding results for periodic wave trains can be derived by integrating over one wave period.

The damping characteristics of a solitary wave, which is a solution of (4.1) with the right-hand side equal to zero, can be computed directly from (4.3). The solitary-wave solution for this special adiabatic case is given by

$$A(\xi,\tau) = \frac{a\lambda^2}{(\xi - v\tau)^2 + \lambda^2}, \tag{4.4}$$

with
$$v = \frac{\gamma}{4}a, \quad \lambda = \left|\frac{4\delta}{\gamma a}\right|.$$

This solution has the properties

$$\langle A \rangle = \pi a \lambda = 4\left|\frac{\delta}{\gamma}\right|, \tag{4.5a}$$

$$\langle A^2 \rangle = \frac{\pi}{2}a^2\lambda = 2\pi a\left|\frac{\delta}{\gamma}\right|. \tag{4.5b}$$

The first property says that the volume of the solitary wave is independent of the amplitude of the wave. Thus, as the wave amplitude decreases, the wavelength increases to preserve the volume. Evaluating (4.3) for this case, we find that

$$\frac{da}{d\tau} = -2\pi\alpha^3|\delta|(a\lambda)^2 f(2\alpha\lambda), \tag{4.6}$$

where
$$f(\beta) = -\frac{d}{d\beta}\int_0^1 (1-t^2)^{\frac{1}{2}} e^{-\beta t}\, dt$$

$$= -\frac{\pi}{2\beta}\{I_0(\beta) - L_0(\beta)\} + \frac{\pi}{\beta^2}\{I_1(\beta) - L_1(\beta)\}. \tag{4.7}$$

The functions $I_n(\beta)$ are the modified Bessel functions of the first kind and the $L_n(\beta)$ are the modified Struve functions. The function $f(\beta)$ has asymptotic forms

$$\lim_{\beta \to 0} f(\beta) = \tfrac{1}{3} - \frac{\pi\beta}{16} + \ldots, \tag{4.8a}$$

$$\lim_{\beta \to \infty} f(\beta) \sim \frac{1}{\beta^2}. \tag{4.8b}$$

Corresponding to these two limiting cases, the decay law for a solitary wave with amplitude a is, respectively,

$$(a_0 - a) = \tfrac{16}{3}\alpha^3 \frac{\delta^2}{|\gamma|}(\tau - \tau_0), \tag{4.9a}$$

$$a = \frac{a_0}{1 + \frac{1}{4}a_0\alpha|\gamma|(\tau - \tau_0)}. \tag{4.9b}$$

Suppose that initially the solitary wave is quite steep ($\alpha\lambda \ll 1$). Then, for fixed α, the wave will begin to decay linearly with time according to (4.9a) and eventually, as λ becomes large to maintain (4.2), the decay will follow (4.9b). For intermediate values of $\alpha\lambda$ or intermediate times, the decay will follow a curve which is a monotonic transition between the above asymptotic results. It is interesting that the damping rate depends quite differently on the coefficient of the nonlinear term γ in the two limits. Of course, these decay laws are only applicable for waves of sufficiently large amplitude so that the ducting condition (2.20) is satisfied. When the amplitude drops below this critical level the wave will disperse throughout the fluid column.

These results can be used to estimate the persistence of long waves propagating in a thermoclinic wave guide. To be specific, consider the case designated by model II(b) in the previous section and shown schematically in table 1. Suppose that a solitary wave with initial amplitude a_0^* is generated and that the appropriate decay law is given by (4.9a). Then the distance, denoted by $x_{\frac{1}{2}}^*$, that the wave travels before decaying to one-half its initial amplitude can be estimated to be

$$\frac{x_{\frac{1}{2}}^*}{\lambda_0^*} \simeq \frac{3}{2}\left(\frac{a_0^*/L}{N_\infty/N_0}\right)^3.$$

The quantity λ_0^* is the initial length of the solitary wave. The environment surrounding the wave guide has a strong influence on the persistence of coherent, long-wave packets.

5. Concluding remarks

The effect of shear on long waves in a stratified flow has been analysed and two types of wave modes have been identified. The first class, those with phase speeds outside the range of flow velocities, reduce to the familiar internal wave modes in the absence of shear when the Richardson number is large. The other class, those with phase speeds within the range of flow velocities, are termed singular modes since the velocity and density perturbations are discontinuous across the critical level where the wave speed matches the flow velocity. We have identified a set of singular modes which are consistent with finite-amplitude waves at high Reynolds numbers so that nonlinearity dominates over viscous and thermal diffusion within a thin layer at the critical level. For a shear layer, this set of singular modes consists of a non-dispersive mode that moves with the mean velocity and an infinite set of discrete modes which are dispersive. The discrete modes have critical levels which are densely packed into the corners of the shear layer. The speed of these wave modes has a peculiar dependence on the location of solid boundaries in the proximity of the shear layer. The waves first speed up as the boundaries are moved away from the shear layer and then slow down again as they become more remote from the layer. One aspect which we have not explored here is the completeness of the set of modes consisting of both the internal wave class and the singular class, and the representation of an arbitrary disturbance in a stratified shear flow with the Richardson number everywhere greater than one-quarter in terms of these modes.

The flow models studied here should prove sufficient to estimate the dependence of long-wave parameters (e.g. the solitary wavenumber) on the Richardson number. They also represent cases where explicit analytical results can be obtained for non-trivial environments. Perhaps the simplest model for assessing the first-order effects of stratification and shear is that of two homogeneous layers of fluid having different density and velocity. Denoting the upper-layer density ρ_1, depth h_1, and velocity

$U_1 = U$ and the lower-layer density $\rho_2 > \rho_1$, depth h_2, and velocity $U_2 = -U$, the amplitude equation for the interfacial displacement $\eta(x,t)$ in the long-wave limit is

$$\eta_t + c_0\eta_x - \frac{3}{2}\frac{1}{h_1 h_2}\frac{\rho_2 h_1^2(U+c_0)^2 - \rho_1 h_2^2(U-c_0)^2}{\rho_1 h_2(U-c_0) - \rho_2 h_1(U+c_0)}\eta\eta_x - \tfrac{1}{6}h_1 h_2 \frac{\rho_1 h_1(U-c_0)^2 + \rho_2 h_2(U+c_0)^2}{\rho_1 h_2(U-c_0) - \rho_2 h_1(U+c_0)}\eta_{xxx} = 0, \tag{5.1}$$

where
$$\frac{c_0}{U} = \frac{\rho_1 h_2 + \rho_2 h_1}{\rho_1 h_2 - \rho_2 h_1} \pm \left\{\frac{1}{U^2}\frac{g(\rho_2-\rho_1)\,h_1 h_2}{\rho_1 h_2 + \rho_2 h_1} - \frac{4\rho_1\rho_2 h_1 h_2}{(\rho_1 h_2 + \rho_2 h_1)^2}\right\}^{\frac{1}{2}}. \tag{5.2}$$

For the evolution equation to be meaningful, the velocity must be small enough to ensure that c_0 is real. At the condition of marginal stability when the bracket term in (5.2) vanishes, the denominator of the coefficients in the evolution equation also vanishes. For these critical shears, the evolution equation is second order in time. In the deep-water limit ($h_2 \to \infty$), the appropriate equation is

$$\eta_t + c_0\eta_x + \frac{3}{2}\frac{U-c_0}{h_1}\eta\eta_x + \tfrac{1}{2}h_1\frac{\rho_2}{\rho_1}\frac{(U+c_0)^2}{U-c_0}\frac{\partial^2}{\partial x^2}\left\{\frac{1}{\pi}\int_{-\infty}^{\infty}\frac{\eta(x',t)}{x-x'}dx'\right\} = 0, \tag{5.3}$$

where
$$\frac{c_0}{U} = 1 \pm \left\{\frac{gh_1(\rho_2-\rho_1)}{\rho_1 U^2}\right\}^{\frac{1}{2}}. \tag{5.4}$$

Using these models, the wavenumber for solitary-wave solutions (cf. equations (3.17) and (4.4)) of these equations has the following dependence on the shear for $|U/c_0| \ll 1$;

$$\left.\begin{aligned} \kappa &= \kappa(U=0)\left\{1 + \frac{2h_1 h_2}{h_1^2 - h_2^2}\frac{U}{c_0} + \ldots\right\}, \\ \kappa &= \kappa(U=0)\left\{1 - 4\frac{U}{c_0} + \ldots\right\}. \end{aligned}\right\} \tag{5.5}$$

These results may be useful in special cases where only the lowest mode is energetic, but information about the higher modes and, in particular, critical-layer modes is totally lacking.

The preceding analysis has also shown how the ambient stratified environment influences the propagation of weakly nonlinear, long internal waves. The (weak) stratification outside the primary thermoclinic wave guide acts as an effective energy sink via wave radiation, thereby limiting the lifetime of ducted wave modes. The stratification external to the wave guide also specifies an amplitude minimum below which long waves cannot remain ducted along the guide. These results place important restrictions on the amplitude and the duration of possible long-wave phenomena to be found in the atmosphere and ocean. However, a converse situation is also suggested, namely that internal waves outside the wave guide may reinforce a wave packet propagating in the wave guide. Although the required conditions are, perhaps, very special for such a favourable interaction, its possibility cannot be ruled out at this stage.

This work was supported by the U.S. National Oceanic and Atmospheric Administration (S.A.M.) and by the Planetary Atmospheres Program of the National

Aeronautics and Space Administration under Grant NGR-05-018-178 (L.G.R.). The first author also acknowledges the support of the J. S. Guggenheim Foundation during the 1978–1979 academic year.

REFERENCES

Abramowitz, M. & Stegun, I. A. 1967 *Handbook of Mathematical Functions*. Washington: National Bureau of Standards.

Apel, J. R., Byrne, H. M., Proni, J. R. & Charnell, R. L. 1975 Observations of oceanic internal and surface waves from the Earth Resources Technology Satellite. *J. Geophys. Res.* **80**, 865–881.

Benjamin, T. B. 1966 Internal waves of finite amplitude and permanent form. *J. Fluid Mech.* **29**, 241–270.

Benjamin, T. B. 1967 Internal waves of permanent form in fluids of great depth. *J. Fluid Mech.* **29**, 559–592.

Benney, D. J. 1966 Long nonlinear waves in fluid flows. *J. Math. Phys.* **45**, 52–63.

Chen, H. H., Lee, Y. C. & Pereira, N. R. 1979 Algebraic internal wave solitons and the integrable Calogero–Moser–Sutherland *N*-body problem. *Phys. Fluids* **22**, 187–188.

Christie, D. R., Muirhead, K. J. & Hales, A. L. 1978 On solitary waves in the atmosphere. *J. Atmos. Sci.* **35**, 805–825.

Davis, R. E. & Acrivos, A. 1967 Solitary internal waves in deep water. *J. Fluid Mech.* **29**, 593–607.

Farmer, D. M. & Smith, J. D. 1978 Nonlinear internal waves in a fjord. *Hydrodynamics of Estuaries and Fjords* (ed. J. Nihoul). Elsevier.

Hadamard, J. 1923 *Lectures on Cauchy's Problem in Linear Partial Differential Equations*. Yale University Press.

Hoiland, E. 1953 On the dynamic effect of variation in density on two-dimensional perturbations of flow with constant shear. *Geophys. Publ.* **18**, no. 10.

Joseph, R. I. 1977 Solitary waves in a finite depth fluid. *J. Phys.* A, *Math. Gen.* **10**, L225–L227.

Keulegan, G. H. 1953 Characteristics of internal solitary waves. *J. Res. Nat. Bur. Stand.* **51**, 133–140.

Kubota, T., Ko, D. R. S. & Dobbs, L. 1978 Weakly-nonlinear, long internal gravity waves in stratified fluids of finite depth. *J. Hydronautics* **12**, 157–165.

Lee, C. & Beardsley, R. 1974 The generation of long nonlinear internal waves in a weakly stratified shear flow. *J. Geophys. Res.* **79**, 453–462.

Long, R. 1965 On the Boussinesq approximation and its role in the theory of internal waves. *Tellus* **17**, 46–52.

Lyra, G. 1943 Theorie der stationären Leewellenströmung in freier Atmosphäre. *Z. angew. Math. Mech.* **23**, 1–28.

Maslowe, S. A. 1972 The generation of clear air turbulence by nonlinear waves. *Stud. Appl. Math.* **51**, 1–16.

Maslowe, S. A. 1973 Finite-amplitude Kelvin–Helmholtz billows. *Boundary-Layer Met.* **5**, 43–52.

Matsuno, Y. 1979 Exact multi-soliton solution of the Benjamin–Ono equation. *J. Phys.* A, *Math. Gen.* **12**, 619–621.

Miles, J. W. 1968 Waves and wave drag in stratified flows. *Proc. 12th Int. Cong. Appl. Mech., Stanford*, pp. 50–75.

Ono, H. 1975 Algebraic solitary waves in stratified fluids. *J. Phys. Soc. Japan* **39**, 1082–1091.

Peters, A. S. & Stoker, J. J. 1960 Solitary waves in liquids having non-constant density. *Comm. Pure Appl. Math.* **13**, 115–164.

Queney, P., Corby, G., Gerbier, N., Koschmieder, H. & Zierep, J. 1960 The airflow over mountains. *World Meteor. Organization, Tech. Note* 34.

Redekopp, L. G. 1977 On the theory of solitary Rossby waves. *J. Fluid Mech.* **82**, 725–745.

Satsuma, J., Ablowitz, M. J. & Kodama, Y. 1980 On an internal wave equation describing a stratified fluid with finite depth. *Phys. Lett.* A (to appear).